Journal of Alloys and Compounds 507 (2010) L21–L25

Contents lists available at ScienceDirect

Journal of Alloys and Compounds

journal homepage: www.elsevier.com/locate/jallcom

Letter

Texture-controlled growth of ZnO nanorods/films by aluminum ion and solvent

Mingsong Wang[a,*], Zhijie Xu[a], Longfei Ge[a], Eui Jung Kim[b,*], Sung Hong Hahn[c], Juan Yang[a], Xiaonong Cheng[a]

[a] School of Materials Science and Engineering, Jiangsu University, Zhenjiang 212013, China
[b] Department of Chemical Engineering, University of Ulsan, Ulsan 680-749, South Korea
[c] Department of Physics, University of Ulsan, Ulsan 680-749, South Korea

ARTICLE INFO

Article history:
Received 14 May 2010
Received in revised form 25 July 2010
Accepted 27 July 2010
Available online 6 August 2010

Keywords:
Zinc oxide
Semiconductors
Chemical synthesis
Crystal growth

ABSTRACT

Great efforts have been made to fabricate ZnO nanostructures/films due to their wide-field applications. In this report, ZnO nanorods/films have been prepared by a low-temperature solution growth. The combined effects of aluminum ion and solvent on the growth of ZnO nanorods/films have been investigated. The density of ZnO nanorods grown in the aqueous solution deceases with increasing concentration of Al^{3+}, while it increases with increasing ethanol content in the solution. The SEM results clearly indicate that there is a competition between solvent and Al^{3+} ion effects on the nucleation density, owing to the lateral growth of ZnO crystals with ethanol and the formation of a second compound of zinc aluminum layered double hydroxide, respectively.

1. Introduction

Zinc oxide (ZnO), a wide band gap II–VI semiconductor, has been extensively investigated due to its useful properties such as optical absorption and emission [1,2], piezoelectricity [3], transparent conductivity [4,5], gas sensitivity [6,7], and photocatalytic activity [8,9]. Numerous works have focused on the fabrication of ZnO in the form of films [2,4,5,7–9] and nanostructures [3,6,10–16]. Among various techniques, solution growth represents an effective and facile way to prepare ZnO nanostructures with well-defined morphologies including nanowires/nanorods [6,10–13], nanoflowers [3,12,14], nanocubes [15], and nanoflakes [16] at a relatively low temperature. A variety of parameters, e.g., types of base [14–16], solvent medium [11], additives of polymers [10] and even inorganic salts [12], can be tuned to direct the shape-controlled growth. So far, one-dimensional (1D) ZnO nanowires/nanorods are intensively studied due to their various applications. Two-step growth has been developed to prepare 1D ZnO nanorod arrays by using seed layer and a subsequent hydrothermal growth [13]. The oriented ZnO nanorods, however, can be tilted by employing a solvent effect, which led to the coalescence of discrete nanorods and the formation of dense thin films [17–20]. By simply controlling the solvent composition, i.e., increasing the volume ratio of ethanol to water in the precursor solution, the crystal orientation ([0 0 1] direction) cab be tuned from perpendicular to almost parallel to the substrate surface [17]. Since tuned crystal orientation leads to the texture-controlled film deposition, understanding the tilting mechanism of crystals is of fundamental and technical interest. Unfortunately, the exact origin is still an open question [18,21].

Al is a well-known *n*-type dopant for ZnO [9,22–24]. Endeavor has been made to incorporate Al into the ZnO nanorods by simply introducing Al salts into the precursor solution [25,26], although this incorporation remains quite difficult because of the different oxidation state, ionic radius and coordination preference between Al^{3+} and Zn^{2+} [27]. On the other hand, it was found that the addition of Al^{3+} to the precursor solution led to the simultaneous preparation of ZnO nanowire/needle arrays on the substrate and a second compound of zinc aluminum layered double hydroxides (ZnAl:LDH) in the bulk solution [28,29]. The formation of ZnAl:LDH competes with the growth of ZnO arrays on the substrate. As a consequence, the density of needle arrays was reduced when Al^{3+} ions were present in the growth solution [30].

Considering the fact that both aluminum ion and solvent affect the film texture regarding the crystal density and orientation, we have investigated the combined effects of aluminum ion and solvent on the growth of ZnO nanorods/films. It is demonstrated that the solvent-controlled film texture is affected significantly by the addition of Al^{3+} ions. A possible mech-

* Corresponding authors. Tel.: +86 511 88780195; fax: +86 511 88791947.
E-mail addresses: wangms@ujs.edu.cn (M. Wang), ejkim@ulsan.ac.kr (E.J. Kim).

0925-8388/$ – see front matter © 2010 Elsevier B.V. All rights reserved.
doi:10.1016/j.jallcom.2010.07.198

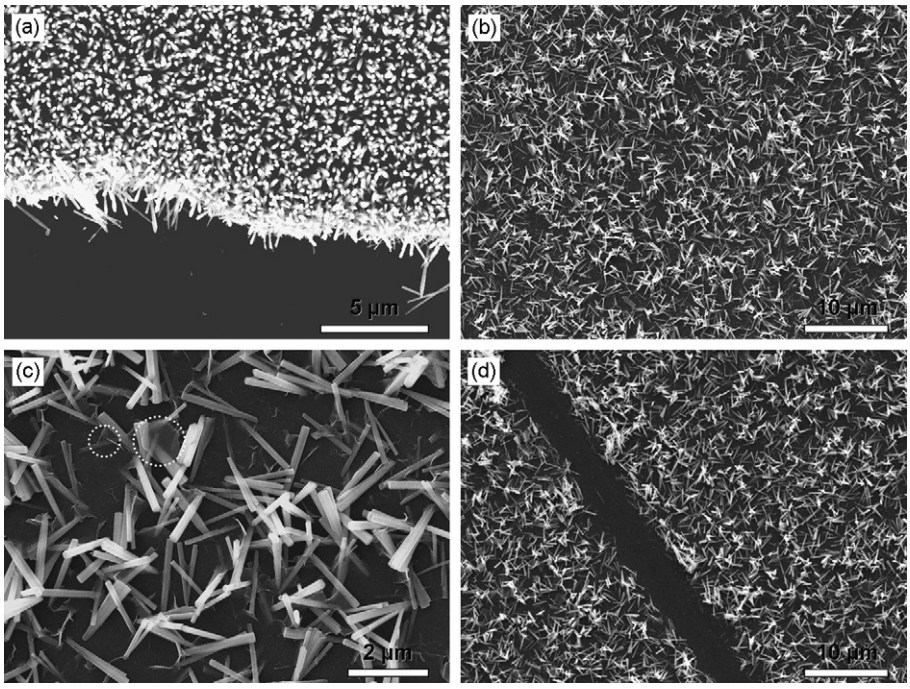

Fig. 1. SEM images of ZnO nanorods grown in the aqueous solution without Al^{3+} (a) and with 10 at.% Al^{3+} (b–d).

anism responsible for the change of film texture has been suggested.

2. Experimental

Solution growth of ZnO nanorods/films was based on our previous works [19]. To promote the heterogeneous growth of ZnO, the glass substrate was pre-coated with a ZnO seed layer by a sol-gel technique. In details, the precursor sol was prepared by dissolving equimolar (0.1 M) zinc acetate ($Zn(CH_3COO)_2{\cdot}2H_2O$, extra pure) and diethanolamine ($HN(CH_2CH_2OH)_2$, extra pure) in ethanol. After dip-coating on the glass substrate, the wet film was annealed at 400 °C for 1 h. For a subsequent hydrothermal growth, a precursor solution was prepared by dissolving 0.137 g zinc acetate and 0.088 g hexamethylenetetramine ($C_6H_{12}N_4$, extra pure) in 50 mL mixed solvent of deionized water and ethanol. The volume ratios of water to ethanol (V_W/V_E) employed in the experiment were 1/0, 1/1, and 1/9 to investigate the solvent effect on the film deposition. The solvent composition is hereafter designated as 0%, 50%, and 90% ethanol. Aluminum ions were added in the form of $Al(NO_3)_3{\cdot}9H_2O$ to the above solution with an Al/Zn molar ratio of 10 and 20 at.%. Glass substrate pre-coated with sol–gel seed layer was immersed in the precursor solution. The synthesis of ZnO nanorods/films was performed at 80 °C for 24 h. After deposition, the samples were rinsed with deionized water and ethanol for several times and finally dried under N_2 flow prior to characterization. Structural characterization was carried out using X-ray diffraction (XRD, Rigaku D/max 2500) with Cu Kα radiation. Sample morphology was examined by a field emission scanning electron microscope (FESEM, JEOL JSM-7001F) operating at an accelerating voltage of 15 kV.

3. Results and discussion

Fig. 1 shows the SEM images of ZnO nanorods grown in the aqueous solution. From Fig. 1(a), it is seen that highly oriented nanorods of 200 nm in diameter and 2.5 μm in length are grown on the seeded glass substrate when no aluminum ions are present in the precursor solution. On the contrary, only sparse nanorods with random orientation are obtained as 10 at.% Al^{3+} ions are added to the precursor solution (Fig. 1(b)). An enlarged image of Fig. 1(b) shows that all nanorods take root in the seed layer and grow out of the substrate surface; the nanorods are quite uniform in shape with their diameter and length of 150 nm and 2 μm, respectively (Fig. 1(c)). Moreover, some flakes are formed together with the nanorods, as indicated by the dashed circles in Fig. 1(c). These flakes may be identified as ZnAl:LDH according to the previous reports [28,29], although only hexagonal ZnO is detected in the XRD spectra possibly due to the trace amount of ZnAl:LDH on the substrate (Fig. 2). We also note that the sparsely distributed nanorods are loosely attached to the substrate; they can be readily removed from the substrate by scratching as indicated in Fig. 1(d). The above results suggest that 1D ZnO nanorods are grown in an aqueous solution regardless of the presence of Al^{3+} ions. The addition of Al^{3+} results in the formation of a second phase, ZnAl:LDH, which competes with the growth of ZnO, thereby leading to the decreased rod density and the increased randomness in rod orientation [30].

The film texture is found to be significantly influenced by the solvent composition. When grown in the 50% ethanol solution without Al^{3+}, dense ZnO films consisting of crystals of ca. 200 nm in size are obtained (Fig. 3(a)). This densification is attributed to the tilting of crystals upon ethanol introduction [17]. However, discrete nanorod arrays are obtained as 10 at.% Al^{3+} ions are added to the 50% ethanol solution (Fig. 3(b)), which are similar in shape to those

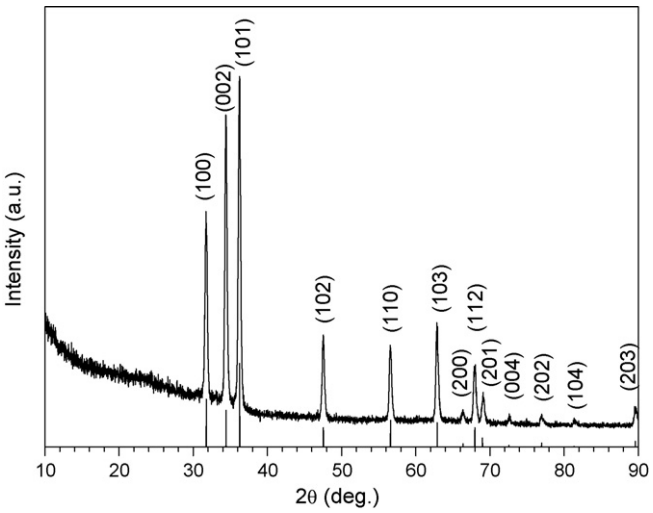

Fig. 2. XRD pattern of ZnO nanorods grown in the aqueous solution with 10 at.% Al^{3+}. All diffraction peaks can be indexed as hexagonal ZnO according to JCPDS 36-1451.

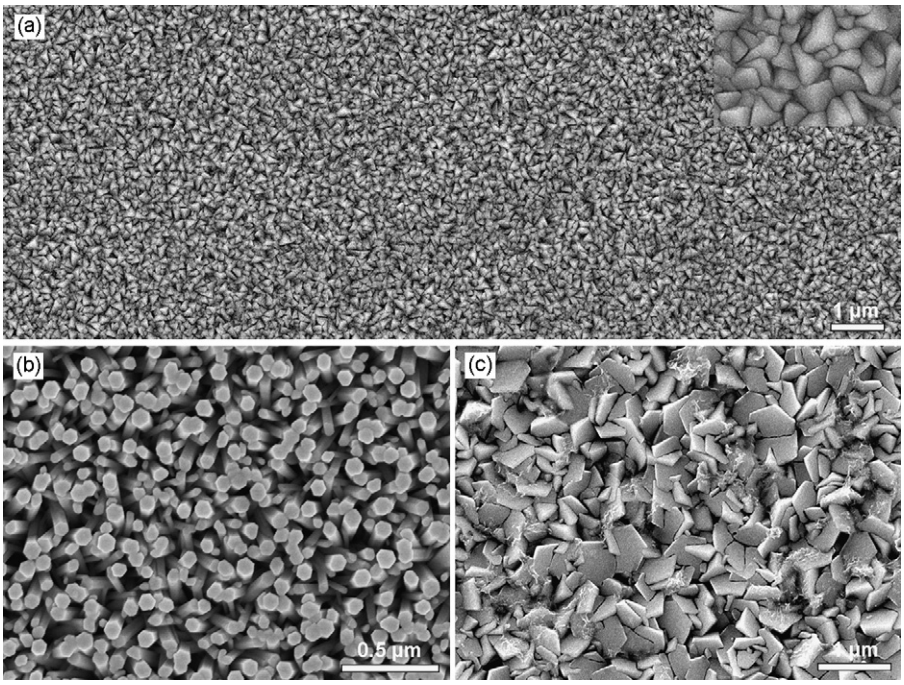

Fig. 3. SEM images of ZnO nanorods/films grown in the 50% ethanol solution without Al^{3+} (a) and with 10 at.% Al^{3+} (b); (c) ZnO films grown in the 90% ethanol solution with 10 at.% Al^{3+}.

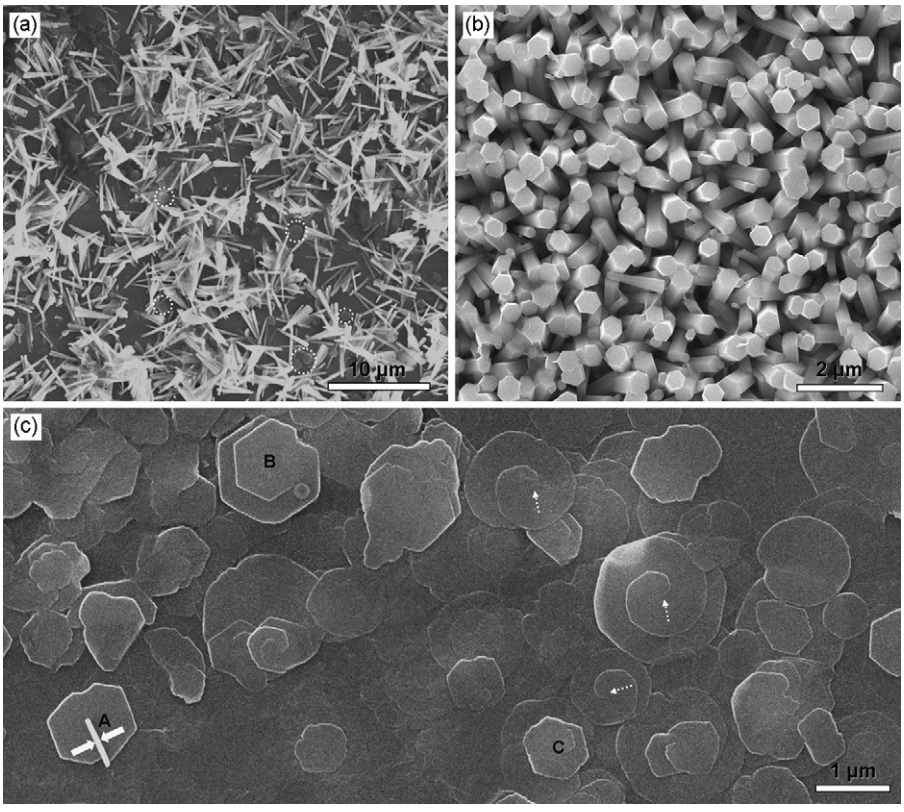

Fig. 4. SEM images of the products grown with 20 at.% Al^{3+} in the aqueous solution (a) and 50% ethanol solution on the seeded glass (b) and bare glass (c).

grown in the aqueous solution shown in Fig. 1(a). Obviously, the crystal tilting due to the solvent effect is inhibited by Al^{3+} ions. Therefore, both solvent and Al^{3+} ion effects play a role in determining the film texture. At a higher ethanol content of 90%, the effect of solvent overwhelms that of Al^{3+} ions, causing the tilting of crystals and resulting in the densification of films (Fig. 3(c)). Nevertheless, the crystal tilting is greatly retarded by the presence of Al^{3+} ions as the (0 0 2) face of the crystals is still observed in Fig. 3(c).

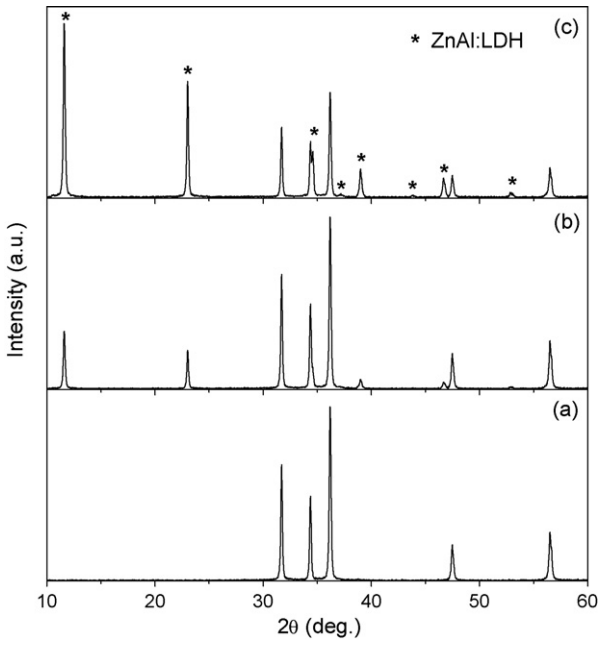

Fig. 5. XRD patterns of the precipitates grown in the aqueous solution with no Al^{3+} (a), 10 at.% Al^{3+} (b), and 20 at.% Al^{3+}. Asterisks (*) indicate the diffraction peaks from ZnAl:LDH.

To further investigate the combined effects of aluminum ion and solvent, the Al^{3+} content is increased to 20 at.% for the solution growth of ZnO nanorods/films. When the deposition is carried out in the aqueous solution, no coatings are formed on the seeded glass in the presence of 20 at.% Al^{3+}. This observation is in agreement with the work by Cho et al. who observed that no ZnO nanoneedles were grown on the seeded substrate at a higher Al^{3+} concentration [30]. Fig. 4(a) shows the SEM image of the white particles precipitated on the substrate, which consist of both ZnO nanorods and ZnAl:LDH disks (indicated by the dashed circles in Fig. 4(a)). The ZnO nanorods have uniform shape with length and diameter of ca. 4 μm and 200 nm, respectively, while the ZnAl:LDH disks are of ca. 1 μm in diameter. In contrast, it is found that uniform coating with faceted ZnO nanorods is grown on the seeded substrate in the 50% ethanol solution even at a high Al^{3+} concentration of 20 at.% (Fig. 4(b)). On the bare substrate, however, only thin ZnAl:LDH disks are formed (Fig. 4(c)). A close look at Fig. 4(c) reveals that some disks (labeled "B" and "C") possess hexagonal configuration, indicating the hexagonal structure of ZnAl:LDH. The spiral-shaped particles indicated by the dashed arrows in Fig. 4(c) suggest that ZnAl:LDH may be grown by screw dislocation. A standing disk labeled "A" shows that the disk thickness is around 60 nm (a lying ZnO nanorod can be excluded as it has much bigger diameter of ca. 500 nm seen in Fig. 4(b).).

As few ZnAl:LDH particles are deposited on the substrate, we have collected the precipitates from bulk solution for XRD measurement. Fig. 5 illustrates the XRD patterns of the precipitates obtained at different Al^{3+} ratios. It is seen therein that pure ZnO is formed when no Al^{3+} is added; however, ZnAl:LDH is synthesized and its phase amount increases with increasing Al^{3+} content up to 20 at.%. Since the atomic ratio of Al to Zn is 39 vs. 61 for such ZnAl:LDH compound [31], it is believed that all Al^{3+} ions participate in the reaction to form ZnAl:LDH, which competes with the growth of ZnO by dissipating Zn^{2+} ions.

The combined effects of aluminum ion and solvent on the texture of ZnO nanorods/films can be explained as follows. Due to the formation of a second phase ZnAl:LDH and its competitive growth with ZnO, the addition of Al^{3+} ions to the precursor solution reduces the number of ZnO nuclei, thus decreasing the rod density on the substrate (Fig. 1(b)). On the other hand, the introduction of ethanol to the aqueous solution suppresses the crystal growth along *c* axis, resulting in the lateral crystallization of ZnO disks [32]. As the crystals are grown on the seeded layer, the disks aggregate by tilting to form dense films consisting of crystal corners. Al^{3+} ions present in the ethanol solution lower the nucleation density of ZnO on the substrate, which effectively prevents the aggregation of crystals and thus facilitates the growth of nanorods (Fig. 3(b), Fig. 4(b)). The addition of ethanol to the aqueous solution with Al^{3+} leads to the lateral growth of ZnO crystals and increases virtually the nucleation density. The growth of dense films (Fig. 3(c)) and fat rods (Fig. 4(b)) is therefore a result of competition between solvent and Al^{3+} ion effects on the nucleation density.

4. Conclusions

In summary, texture-controlled growth of ZnO nanorods/films has been demonstrated using combined effects of aluminum ion and solvent. When grown in the solution with ethanol, dense films consisting of crystal corners are formed due to the aggregated crystal growth on the seeded layer. If Al^{3+} ions are present in the ethanol solution, they lower the nucleation density of ZnO on the substrate, which effectively prevents the aggregation of crystals and facilitates the growth of nanorods. The growth of ZnO films/nanorods is a result of competition between solvent and Al^{3+} ion effects on the nucleation density.

Acknowledgements

This work was supported by the Research Foundation of Jiangsu University (No. 09JDG004) and the National Natural Science Foundation of China (No. 50902061).

References

[1] D. Jin, N. Liao, X. Xu, X. Yu, L. Wang, L. Wang, Mater. Chem. Phys. 123 (2010) 363–366.
[2] M. Gao, J. Liu, H. Sun, X. Wu, D. Xue, J. Alloys Compd. 500 (2010) 181–184.
[3] M.K. Gupta, N. Sinha, B.K. Singh, N. Singh, K. Kumar, B. Kumar, Mater. Lett. 63 (2009) 1910–1913.
[4] B. Zhang, B. Yao, S. Wang, Y. Li, C. Shan, J. Zhang, B. Li, Z. Zhang, D. Shen, J. Alloys Compd. 503 (2010) 155–158.
[5] R. Deng, B. Yao, Y.F. Li, T. Yang, B.H. Li, Z.Z. Zhang, C.X. Shan, J.Y. Zhang, D.Z. Shen, J. Cryst. Growth 312 (2010) 1813–1816.
[6] M.-W. Ahn, K.-S. Park, J.-H. Heo, D.-W. Kim, K.J. Choi, J.-G. Park, Sensor Actuator B 138 (2009) 168–173.
[7] A.U. Ubale, V.P. Deshpande, J. Alloys Compd. 500 (2010) 138–143.
[8] N. Kaneva, I. Stambolova, V. Blaskov, Y. Dimitriev, S. Vassilev, C. Dushkin, J. Alloys Compd. 500 (2010) 252–258.
[9] M. Bizarro, Appl. Catal. B 97 (2010) 198–203.
[10] P.G. Li, S.L. Wang, W.H. Tang, J. Alloys Compd. 489 (2010) 566–569.
[11] Q.R. Hu, S.L. Wang, P. Jiang, H. Xu, Y. Zhang, W.H. Tang, J. Alloys Compd. 496 (2010) 494–499.
[12] R. Yi, H. Zhou, N. Zhang, G. Qiu, X. Liu, J. Alloys Compd. 479 (2010) L50–L53.
[13] L. Vayssieres, Adv. Mater. 15 (2003) 464–646.
[14] Q. Li, H. Sun, M. Luo, W. Weng, K. Cheng, C. Song, P. Du, G. Shen, G. Han, J. Alloys Compd. 503 (2010) 514–518.
[15] L. Yu, F. Qu, X. Wu, J. Alloys Compd. 504 (2010) L1–L4.
[16] X. Xu, C. Cao, J. Alloys Compd. 501 (2010) 265–268.
[17] M. Wang, E.J. Kim, E.W. Shin, J.S. Chung, S.H. Hahn, C. Park, J. Phys. Chem. C 112 (2008) 1920–1924.
[18] M. Wang, E.J. Kim, S.H. Hahn, C. Park, K.-K. Koo, Cryst. Growth Des. 8 (2008) 501–506.
[19] M. Wang, S.H. Hahn, E.J. Kim, J.S. Kim, S. Kim, C. Park, K.-K. Koo, Thin Solid Films 516 (2008) 8599–8603.
[20] M. Wang, S.H. Hahn, J.S. Kim, S.H. Hong, K.-K. Koo, E.J. Kim, Mater. Lett. 62 (2008) 4532–4534.
[21] Th. Pauporté, Cryst. Growth Des. 7 (2007) 2310–2315.
[22] J.-S. Na, G. Scarel, G.N. Parsons, J. Phys. Chem. C 114 (2010) 383–388.
[23] G.G. Rusu, A.P. Râmbu, V.E. Buta, M. Dobromir, D. Luca, M. Rusu, Mater. Chem. Phys. 123 (2010) 314–321.
[24] E. Bacaksiz, S. Aksu, S. Yılmaz, M. Parlak, M. Altunbaş, Thin Solid Films 518 (2010) 4076–4080.
[25] S. Yun, J. Lee, J. Yang, S. Lim, Physica B 405 (2010) 413–419.

[26] M. Eskandari, V. Ahmadi, S.H. Ahmadi, Physica E 42 (2010) 1683–1686.
[27] H. Serier, M. Gaudon, M. Ménétrier, Solid State Sci. 11 (2009) 1192–1197.
[28] G. Hua, Y. Tian, L. Yin, L. Zhang, Cryst. Growth Des. 9 (2009) 4653–4659.
[29] S. Cho, S.-H. Jung, J.-W. Jang, E. Oh, K.-H. Lee, Cryst. Growth Des. 8 (2008) 4553–4558.
[30] S. Cho, B.R. Lee, H.-J. Kim, D.-H. Park, K.-H. Lee, Mater. Lett. 63 (2009) 2025–2028.
[31] M.S. Yarger, E.M.P. Steinmiller, K.-S. Choi, Inorg. Chem. 47 (2008) 5859–5865.
[32] M. Wang, S.H. Hahn, J.S. Kim, J.S. Chung, E.J. Kim, K.-K. Koo, J. Cryst. Growth 310 (2008) 1213–1219.